



# Non-Invasive Monitoring of HER2 Expression in Breast Cancer Patients with $^{99m}\text{Tc}$ -Affibody SPECT/CT

Jiong Cai<sup>1,\*</sup>, Xin Li<sup>2</sup>, Feng Mao<sup>3</sup>, Pan Wang<sup>1</sup>, Yaping Luo<sup>4</sup>, Kun Zheng<sup>4</sup>, Fang Li<sup>4</sup> and Zhaohui Zhu<sup>4</sup>

<sup>1</sup>Department of Nuclear Medicine, Affiliated Hospital of Zunyi Medical University, Zunyi, China

<sup>2</sup>Department of Nuclear Medicine, Zhejiang Cancer Hospital, Hangzhou, China

<sup>3</sup>Department of Breast Surgery, Peking Union Medical College Hospital, Chinese Academy of Medical Sciences and Peking Union Medical College, Beijing, China

<sup>4</sup>Department of Nuclear Medicine, Peking Union Medical College Hospital, Chinese Academy of Medical Sciences and Peking Union Medical College, Beijing, China

\*Corresponding author: Department of Nuclear Medicine, Affiliated Hospital of Zunyi Medical University, Zunyi, China. Email: jiongcai@sina.com

Received 2019 July 17; Revised 2019 November 16; Accepted 2019 November 27.

## Abstract

**Background:** Non-invasive monitoring of human epidermal growth factor receptor 2 (HER2) status in malignant lesions of breast cancer patients has been established in clinical positron emission computed tomography (PET).

**Objectives:** In this study, we try to evaluate the feasibility of  $^{99m}\text{Tc}$ -labeled affibody in monitoring HER2 expression for breast cancer patients using single-photon emission computed tomography (SPECT) apparatus fused with a conventional CT scanner (SPECT/CT).

**Patients and Methods:** HER2 affibody with endogenous chelating site was recombinantly expressed and purified.  $^{99m}\text{Tc}$  was added to HER2 affibody at carboxyl-terminal cystein site specifically. Breast cancer patients were enrolled for whole-body SPECT/CT imaging following intravenous administration of  $^{99m}\text{Tc}$ -labeled HER2 affibody. Regions of interest were drawn manually over tumor sites and the normal surrounding muscle. The HER2 status of breast cancer lesions was determined by post-surgical immunohistochemistry, and correlated with the uptake of  $^{99m}\text{Tc}$ -labeled affibody as measured by SPECT.

**Results:** Administration of  $^{99m}\text{Tc}$ -labeled HER2 affibody was well tolerated by all patients without noticeable adverse side effects.  $^{99m}\text{Tc}$ -labeled affibody SPECT imaging clearly visualized HER2 positive breast cancer lesions at approximately 1.5 and 4.5 hours after affibody treatment. The tumor to background (T/B) ratios of locally hot breast cancer lesions by HER2 imaging were closely related to post-surgical HER2 expression levels of cancer tissues by immunohistochemistry. When the tumor:muscle ratio exceeded 2.4 (cutoff value) in transverse imaging, the tumor lesion was considered to be HER2-positive arbitrarily. The diagnostic sensitivity of  $^{99m}\text{Tc}$ -labeled affibody SPECT/CT in identifying HER2 positive breast cancer was 80 percent (12/15), while the specificity and accuracy of  $^{99m}\text{Tc}$ -labeled affibody SPECT/CT were 60 percent (9/15) and 70 percent (21/30) respectively. In tumors with a diameter greater than 12 mm, the sensitivity of  $^{99m}\text{Tc}$ -labeled affibody SPECT/CT was 100 percent (12/12).

**Conclusion:**  $^{99m}\text{Tc}$ -labeled affibody SPECT/CT may find utility in evaluating HER2 expression in breast cancer patients, and may provide new modality for guiding HER2 targeted therapy complementary to biopsy in breast cancer.

**Keywords:**  $^{99m}\text{Tc}$ , SPECT/CT, HER2, Affibody, Breast Cancer

## 1. Background

Breast cancer (BC) is the most common malignant tumor, leading to one fourth of cancer population in women among all presenting types of cancer (1). Human epidermal growth factor receptor type 2 (HER2) is frequently over-expressed in breast cancer (2), and is crucial in predicting survival and the effectiveness of HER2-targeted therapy (3-10). The level of HER2 expression could be determined by immunohistochemistry (IHC) and fluorescence in situ hybridization (FISH) of tumor samples (11, 12). However, previous data has demonstrated a discordance of about 20% between HER2 protein expression in primary tumors and tumors that have metastasized to the local lymph nodes (13-

15) as determined by IHC or FISH. Thus, there is an urgent need to develop non-invasive imaging of HER2 status in both primary and synchronous axillary lymph node metastasis for accurate HER2 diagnosis.

Single-photon emission computed tomography (SPECT) was used to profile and delineate the radioactivity distributions within the body to probe its physiological and chemical processes. Radiolabeled antibodies, antibody fragments, affibodies and peptides have been used to design reliable and quantitative radiotracers to target HER2 for nuclear imaging (16-24). Although monoclonal antibodies have been traditionally used as tracing agents for HER2 in preclinical tests, the slow uptake in tumors

and sustained retention in the circulation make it problematic for prompt localization of the target when they are conjugated with radio-isotopes as SPECT tracers (16). In contrast, HER2 affibodies can efficiently penetrate tumors, following which, they are rapidly cleared from the blood (25).

An affibody is a molecule that is structurally based on a non-immunoglobulin scaffold from the Z domain of protein A, which is a surface protein of the bacterium *Staphylococcus aureus* (26). In terms of its binding features, an affibody mimics a monoclonal antibody and can bind to HER2 with high affinity and specificity. In terms of size, an affibody only has a molecular weight of 6 kDa, which is far less than a monoclonal antibody of a molecular weight of 150 kDa. In terms of its stability, an affibody can withstand a variety of conjugation conditions, including extreme ranges of pH and elevated temperatures (27).

The technological approach of radiolabeled affibody has been used to detect HER2-positive cancer using the SPECT and positron emission computed tomography (PET) (18-24), which permits HER2 imaging in animal models and human subjects using Indium-111 (<sup>111</sup>In) for SPECT and <sup>68</sup>Ga, <sup>18</sup>F for PET within 24 hours of administering the radio-labeled probe (28-32). Although <sup>99m</sup>Tc is the most widely used nuclide for SPECT imaging that displays both an ideal gamma energy (140 KeV) and commercial availability (25), there are no clinical reports that have described the use of <sup>99m</sup>Tc labeled HER2 affibody in the current literature at this time. Zhang et al. labeled HER2 affibody with a <sup>99m</sup>Tc and tested its imaging properties in a HER2-expressing SKOV-3 xenografted murine model (25). Wallberg et al. selected a HER2 affibody that incorporated the C-terminal GGGC chelator for <sup>99m</sup>Tc labeling after evaluating several alternative HER2 affibody variants that incorporated the C-terminal GGSC, GGEC, GGKC or GSEC chelators. This optimal variant provided the lowest radioactive retention across all normal/unaffected organs and tissues including the kidneys in SKOV-3 xenografted mice (33).

## 2. Objectives

In the current study, HER2 affibody with endogenous chelating site was recombinantly expressed and purified. <sup>99m</sup>Tc was added to HER2 affibody at carboxyl-terminal cystein site-specifically. We tested the feasibility of this <sup>99m</sup>Tc-labeled HER2-specific affibody construct to image HER2-positive breast cancer in patients by the SPECT-CT approach. After SPECT imaging, the status of HER2 expression in breast cancer lesions was quantified by HER2 immunohistochemical staining during surgery. In addition, HER2 expression levels were correlated with the uptake of <sup>99m</sup>Tc-labeled affibody as measured by SPECT.

## 3. Patients and Methods

This study was performed according to the declaration of Helsinki ethical standards for experiments with humans and approved by Peking Union Medical College Hospital Ethical Committee of the Chinese Academy of Medical Sciences (protocol number JS-893). The protocol is also registered at: www.ClinicalTrials.gov (NCT 03546478). In addition, written and informed consent was obtained from each patient.

### 3.1. HER2 Affibody Recombinant Expression and Purification

The HER2 affibody had an amino acid sequence of EHEHEAENKFNKEMRNAYWEIALLPNLTNQKRAFIRSLYDDP-SQSANLLAEAKKLNDAAQGGGC and was used for endogenous labeling with <sup>99m</sup>Tc (27). The modified HER2 affibody gene was cloned into the pET22b (+) plasmid and transformed into competent BL21 (DE3) bacteria for recombinant DNA expression. The affibody was further purified using nickel affinity chromatography and identified by sodium dodecyl-sulfate polyacrylamide gel electrophoresis (SDS-PAGE) (27, 34).

### 3.2. Preparation of <sup>99m</sup>Tc-labeled HER2 Affibody

The <sup>99m</sup>Tc-labeled HER2 affibody was synthesized in a sterile hot chamber. Briefly, the affibody was diluted in phosphate buffered saline (PBS) to a concentration of 0.8 mg/mL and stored at -20°C before use. Fresh <sup>99m</sup>Tc was eluted into a sterile vacuum bottle from the <sup>99</sup>Mo/<sup>99m</sup>Tc generator using 5 mL of sterile saline. Two hundred microliters of <sup>99m</sup>TcO<sub>4</sub><sup>-</sup> (1.11 - 1.85 gigabecquerel [GBq]) was drawn for labeling from the bottle. Fifty microliter of the affibody was added to 200 μL of the degassed buffer (pH 6.6) containing 20 mmol/L sodium glucoheptonate and 10 mmol/L 4-(2-hydroxyethyl)-1-piperazineethane sulfonic acid (HEPES) in a 1.5 mL microtube, following which, 50 μg Tin (II) chloride (SnCl<sub>2</sub>) in 1 μL of 10% hydrochloric acid (HCl) and <sup>99m</sup>Tc were added. The mixture was kept at room temperature for an additional 10 minutes, and then further purified by NAP-5 gravity flow column (GE healthcare, USA). A 0.22 μm sterile ultrafine filter was then used for sterility purification.

### 3.3. Quality Control of <sup>99m</sup>Tc-labeled HER2 Affibody

Instant thin-layer chromatography (ITLC) (Bioscan 2000, USA) was used to test radio-chemical purity (RCP) and <sup>99m</sup>Tc-radiocolloid, and ITLC-silics gel (SG) strips (Gelman, USA) were used as the solid phase support (33). For RCP determination, PBS (10 mM) was used as the developing solution, the retention factor (Rf) value of the <sup>99m</sup>Tc labeled affibody was 0, and that of pertechnetate and glucoheptonate complexes of <sup>99m</sup>Tc was 1. For radiocolloid determination, a solution of 53% pyridine and 32% acetic acid

was used as the developing solution, the Rf value of any technetium colloid was 0 and that of the  $^{99m}\text{Tc}$  labeled affibody, pertechnetate or other complexes of  $^{99m}\text{Tc}$  was 1. For clinical use, the RCP of the  $^{99m}\text{Tc}$ -labeled HER2 affibody was always greater than 95 percent and the technetium colloid was usually below 0.5 percent.

#### 3.4. *In Vitro* Characterization of $^{99m}\text{Tc}$ -labeled HER2 Affibody

For *in vitro* characterization, MDA-MB-361 breast cancer cells (HER2 positive) were cultured with L15 medium containing fetal bovine serum (20%), penicillin (100 U/mL) and streptomycin (100  $\mu\text{g}/\text{mL}$ ). The day before the binding test, one million MDA-MB-361 breast cancer cells that were suspended in two milliliters of L15 medium were dropped into each well of a six-well plate. The next day, the  $^{99m}\text{Tc}$ -labeled HER2 affibody (19.2 GBq/ $\mu\text{mol}$ ) was added to the wells with different final concentrations of 0.0004, 0.0021, 0.011, 0.054, 0.260, 1.310, 6.7, and 33 nmol/L in triplicate. The blocking wells were occupied with a 50-fold concentration of "cold" HER2 affibody and the  $^{99m}\text{Tc}$ -labeled HER2 affibody. All radioactive wells were incubated at 4°C for 2 hours for cell binding, then washed with ice-cold PBS three times and detached with trypsin buffer. The radioactivity of the  $^{99m}\text{Tc}$ -labeled HER2 affibody that was bound to the cells was measured by a gamma counter.

#### 3.5. *In Vivo* Characterization of $^{99m}\text{Tc}$ -labeled HER2 Affibody in Breast Cancer Models

For *in vivo* characterization, ten BALB/c nude mice were used for xenograft cancer modeling. Ten million MDA-MB-361 breast cancer cells in 50  $\mu\text{L}$  of culture medium were mixed with the same volume of Matrigel (BD Sci., USA) and simultaneously seeded into each mouse axilla. When the diameter of the tumor was 5 mm, the  $^{99m}\text{Tc}$ -labeled HER2 affibody was prepared as described above, and administered into the mouse tail vein with a single dose of 37 MBq ( $\sim 0.36$  nmol) in 0.2 mL of saline. Whole-body imaging of  $^{99m}\text{Tc}$ -labeled HER2 affibody in breast cancer models was obtained at 1.0 and 4.5 hours post-injection for 20 minutes with the NanoSPECT/CT apparatus (Mediso, Hungary) under 10 percent chloral hydrate anesthesia (4  $\mu\text{L}/\text{g}$  body weight) given intraperitoneally. The *in vivo* specific binding of the  $^{99m}\text{Tc}$ -labeled HER2 affibody was further confirmed by pre-injection of 200  $\mu\text{g}$  of "cold" HER2 affibody and 37 MBq of  $^{99m}\text{Tc}$ -labeled HER2 affibody two days later using the same mouse models and the same acquisition methods. CT was used to locate the tumor, and the heart, liver, lung, muscle, humeral bone and the brain. The In Vivo Scope Browser software was used to analyze focal radioactivity by manual drawing transversely for calculation of the target to non-target (T/NT) ratio.

#### 3.6. Patient Enrollment

To study the diagnostic value of  $^{99m}\text{Tc}$ -labeled HER2 affibody SPECT/CT, female patients were continuously enrolled from July 10 through November 20, 2015. The inclusion criteria included the following: an age of 28 years or older, suspected diagnosis of HER2-positive breast cancer, being able to provide specific disease information, and understanding the nature and importance of informed consent. The exclusion criteria included the following considerations: pregnancy, lactation, kidney failure, liver dysfunction, claustrophobia, and post mastectomy.

#### 3.7. $^{99m}\text{Tc}$ -labeled HER2 Affibody Imaging in Breast Cancer Patients

Each patient was injected with  $5.6 \pm 0.8$  MBq of the  $^{99m}\text{Tc}$ -labeled HER2 affibody per kilogram (which was equivalent to approximately 50  $\mu\text{g}$ ) via the left basilic vein at the cubital fossa. Following intravenous injection of the  $^{99m}\text{Tc}$ -labeled HER2 affibody, anterior and posterior SPECT scans of the whole body were acquired at 1.5 and 4.5 hours time-points for 20 minutes with a scanner equipped with dual-head  $\gamma$ -cameras and high-resolution collimators for low-energy gamma rays detection (Precedence, ADAC laboratories of Philips, USA). The SPECT scans were fused to CT scans for accurate localizing anatomical structure. All digital imaging data of breast cancer patients were transferred to a center workstation for detailed reading and analysis. In a fraction of the studied patients,  $^{18}\text{F}$ -fluorodeoxyglucose ( $^{18}\text{F}$ -FDG) PET was undertaken as a control.

#### 3.8. HER2 Immunohistochemical Staining

Lumpectomy was done under general anesthesia. Briefly, an incision was made to the breast with the intention of removing the tumor, along with a small rim of normal tissue that was located about the site of the tumor, in addition to lymph nodes in the underarm area. Representative tumor and lymph node samples that were obtained during surgery were fixed with neutral formalin for 2 days, then dehydrated with serial concentrations of alcohol, xylene and finally embedded tissues with paraffin wax (56 - 58°C) in blocks. Five-micrometer ( $\mu\text{m}$ ) thick tissue sections were cut and mounted on glass slides. The endogenous peroxidase in sections were blocked with 3%  $\text{H}_2\text{O}_2$  for 10 minutes and washed with PBS containing 1% bovine serum albumin (BSA) for three times. The blocked tissues were added with a mouse monoclonal antibody (Clone UMAB36, Origene, USA) that was raised against HER2 (1:200) and incubated at 37°C for 2 hours. After washing with PBS, the sections were incubated with secondary antibody (horseradish peroxidase [HRP]-conjugated, goat

anti-mouse IgG) at room temperature for 30 minutes. After thorough washing, the tissues were added with 3% diaminobenzidine and 0.3% H<sub>2</sub>O<sub>2</sub> for color development. Light microscopy was used to observe stained tissues and six fields of each section were randomly chosen for analysis by the same pathologist with a track-record of more than 15 years of experience.

### 3.9. Data Analysis

SPECT images were analyzed by two experienced researchers. The sources of SPECT and CT images were masked to these researchers. In visual characterization, the different organ images, number of lesions, and imaging time-points were documented. The number of lesions included primary lesions and lymph node metastases. For quantitative determination, the 4.5 h images were adopted for analysis because these images were better than 1.5 h images. The radioactivity of the <sup>99m</sup>Tc-labeled affibody uptake in breast cancer lesions and the surrounding muscle were measured and the tumor-to-background (T/B) ratios of SPECT images at the 4.5 h time-point were calculated by the same researchers.

### 3.10. Statistical Analysis

The dissociation constant (Kd) was calculated by specific binding of <sup>99m</sup>Tc-labeled HER2 affibody to HER2 positive cells (total binding minus nonspecific binding) with GraphPad Prism 5 software (CA, USA). The sensitivity, specificity, and accuracy values (%) of <sup>99m</sup>Tc-labeled affibody in diagnosing HER2 positive breast cancer were also calculated with GraphPad Prism 5 software. Uni-variate analysis enabled correlating SPECT imaging of the T/B ratios and HER2 IHC grades.

## 4. Results

### 4.1. In Vitro Characterization of the <sup>99m</sup>Tc-labeled HER2 Affibody

The <sup>99m</sup>Tc-labeled HER2 affibody bound to MDA-MB-361 breast cancer cells specifically with a Kd value of 1.7 nmol/L. The final purified mass concentration was 0.5 mg/mL. The synthesis time of the <sup>99m</sup>Tc-labeled HER2 affibody was usually less than 20 minutes. The labeling yield and final RCP were 99.5 ± 0.3 percent. The RCP of <sup>99m</sup>Tc-labeled HER2 affibody were 98.4 ± 0.2 percent and 96.3 ± 0.7 percent respectively after 3 hours incubation at 37°C with PBS and serum, and were 98.1 ± 0.6 percent and 95.0 ± 1.0 percent respectively after 6 hours incubation at 37°C with PBS and serum, which indicate <sup>99m</sup>Tc- affibody was stable both in PBS and serum.

### 4.2. In Vivo Characterization of the <sup>99m</sup>Tc-labeled HER2 Affibody

The MDA-MB-361 mouse model of a breast cancer xenograft was clearly visualized by the NanoSPECT/CT at 1.0 hours and 4.5 hours after <sup>99m</sup>Tc- labeled HER2 affibody injection (Figure 1A and B). The radioactivity in the thyroid gland was negligible. By contrast, the radioactivity in the kidney and urinary bladder was prominent, which indicated that the urinary tract served as the main excretion pathway for <sup>99m</sup>Tc- labeled HER2 affibody. In the blocking group with “cold” HER2 affibody, the MDA-MB-361 breast cancer xenograft was not clearly visualized at both 1.0 hrs and 4.5 hrs after <sup>99m</sup>Tc- labeled HER2 affibody injection (Figure 1C and D). The T/NT ratios of the cancer to the heart, liver, lung, muscle, bone and brain were 7.61 ± 0.56, 1.81 ± 0.60, 8.95 ± 1.13, 10.62 ± 1.78, 11.42 ± 2.07, and 20.08 ± 6.12, respectively. In the blocking group, the T/NT ratios of the cancer to the heart, liver, lung, muscle, bone and brain were decreased to 2.42 ± 1.02, 0.60 ± 0.23, 3.05 ± 1.38, 8.16 ± 2.66, 2.76 ± 0.48, and 5.24 ± 2.17, respectively (F = 29.38; P < 0.05).

### 4.3. Evaluation of Patients with Suspected Breast Cancer

Information regarding a detailed pathological diagnosis of all patients following SPECT/CT imaging is described in Table 1. For SPECT/CT imaging, 30 female patients (aged 29 - 76 years; mean, 48.2 ± 11.1 years) with suspected HER2-positive breast cancer were enrolled into the study. In patient No. 1, primary lesions and lymph node metastases could be clearly seen by <sup>99m</sup>Tc-labeled affibody SPECT/CT imaging (Figure 2A and B). Positive primary tumor foci could be clearly observed between 1.5 to 4.5 hours after intravenous injection of the <sup>99m</sup>Tc-labeled affibody. At the 4.5 hours time-point, a HER2 positive lesion was optimally visible by maximum intensity projection (MIP) imaging than at the 1.5 hours time-point (T/B: 6.0 ± 5.6 vs. 4.6 ± 4.1, P < 0.05). <sup>99m</sup>Tc-labeled affibody accumulated in primary lesions with a very high T/B ratio (23.8 ± 2.9), while the lymph node metastases were also HER2 positive. The T/B ratios of the axillary lymph nodes and supraclavicular lymph nodes were high (i.e., 6.5 ± 1.4 and 6.1 ± 1.3 respectively; Figure 2C-E). MIP images (Figure 2A and B) showed that breast cancer cells migrated from the right breast duct to the axillary and supraclavicular lymph nodes. HER2-positive lesions were clearly located when the SPECT images fused with the traditional CT images. In the transverse plane, the radioactivity that was measured in the breast cancer lesion was higher than that quantified in the heart (T/B ratio = 1.5 ± 0.9) and normal breast tissues (T/B ratio = 1.0 ± 0.2) (Figure 2C), which indicated that the <sup>99m</sup>Tc-labeled affibody was specifically bound to the HER2 target in the circulation. In the coronal plane, the radioactivity in the liver (T/B ratio = 21.9

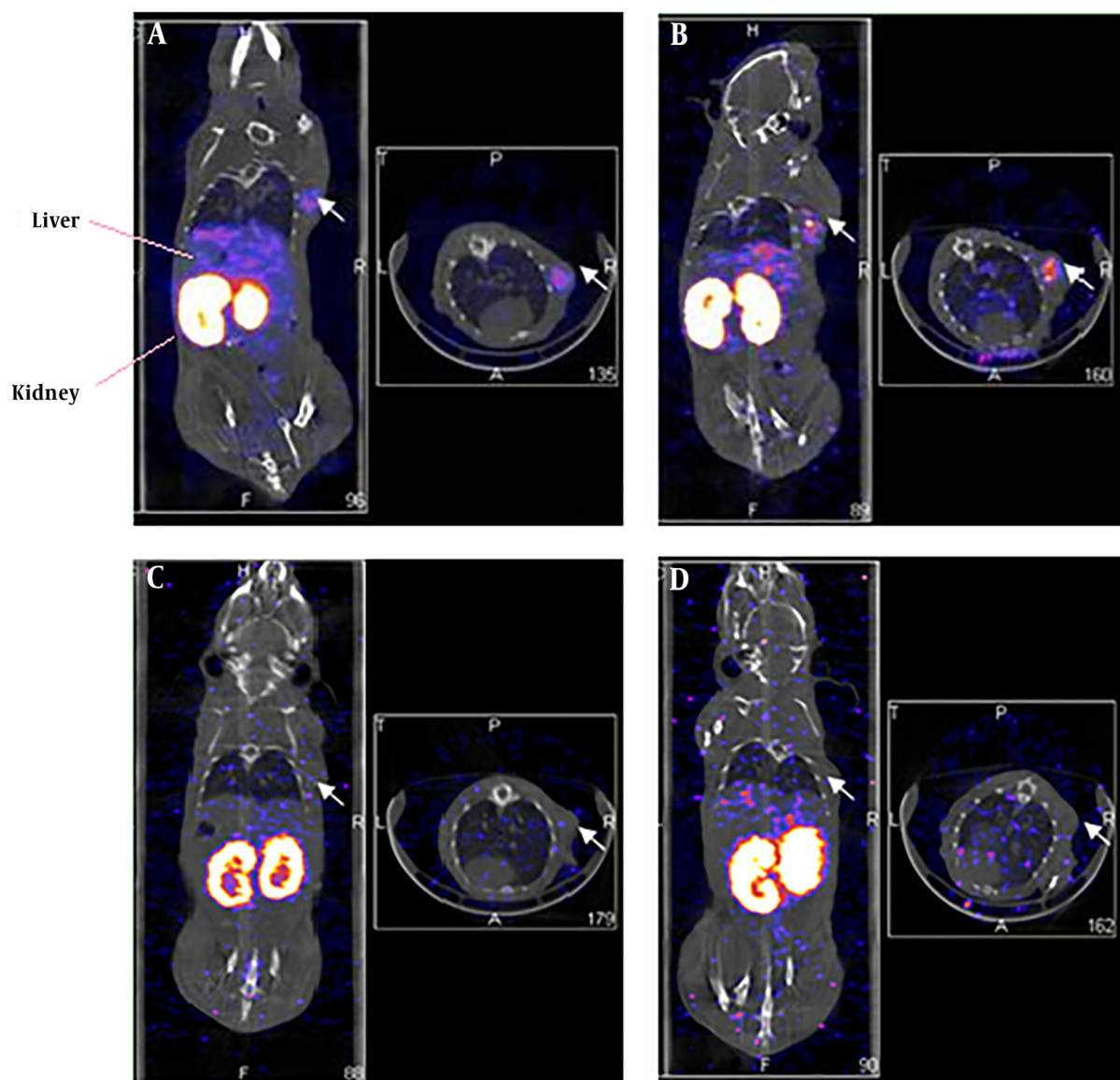


**Figure 1.** Single-photon emission computed tomography (SPECT)/CT imaging of  $^{99m}\text{Tc}$ -labeled human epidermal growth factor receptor 2 (HER2) affibody in human HER2-positive breast carcinoma in xenografted mice (left: coronal plane; right: transverse plane). A and B, Images of  $^{99m}\text{Tc}$ -ABH2 at 1h (A) and 4.5h (B), white arrows point radioactivity accumulated MDA-MB-361 breast carcinoma. C and D, Blocking images of  $^{99m}\text{Tc}$ -ABH2 at 1h (C) and 4.5h (D), radioactivity was not accumulated in MDA-MB-361 breast carcinoma.

$\pm 3.5$ ) was comparable with that found in the breast lesion. By contrast, the radioactivity measured in the kidneys ( $57.3 \pm 14.6$ ) was much higher than that measured in the breast lesions (Figure 2F). In the sagittal plane, uptake of radioactivity by the breast cancer lesion was prominent (Figure 2G). The primary lesion and lymph node metastases were surgically resected and histologically evaluated and diagnosed as invasive ductal carcinoma. IHC results indicated that the primary lesion and lymph node metastases were all HER2 3+ (Figure 2H and I).

In contrast, some of the HER2 negative primary breast cancers with/without lymph node metastases did not retain the  $^{99m}\text{Tc}$ -labeled affibody when analyzed by SPECT/CT imaging. The  $^{99m}\text{Tc}$ -labeled affibody SPECT/CT imaging in patient No. 22 showed that uptake of radioactivity in the left breast nodule was very low (T/B ratio =  $0.8 \pm 0.1$ ), and was comparable to that found in the muscle (T/B ratio =  $0.9 \pm 0.2$ ) and lung (T/B ratio =  $0.7 \pm 0.1$ ) (Figure 3A). Post-surgical IHC staining indicated that this invasive ductal carcinoma was HER2 negative (Figure 3B). In addition, the

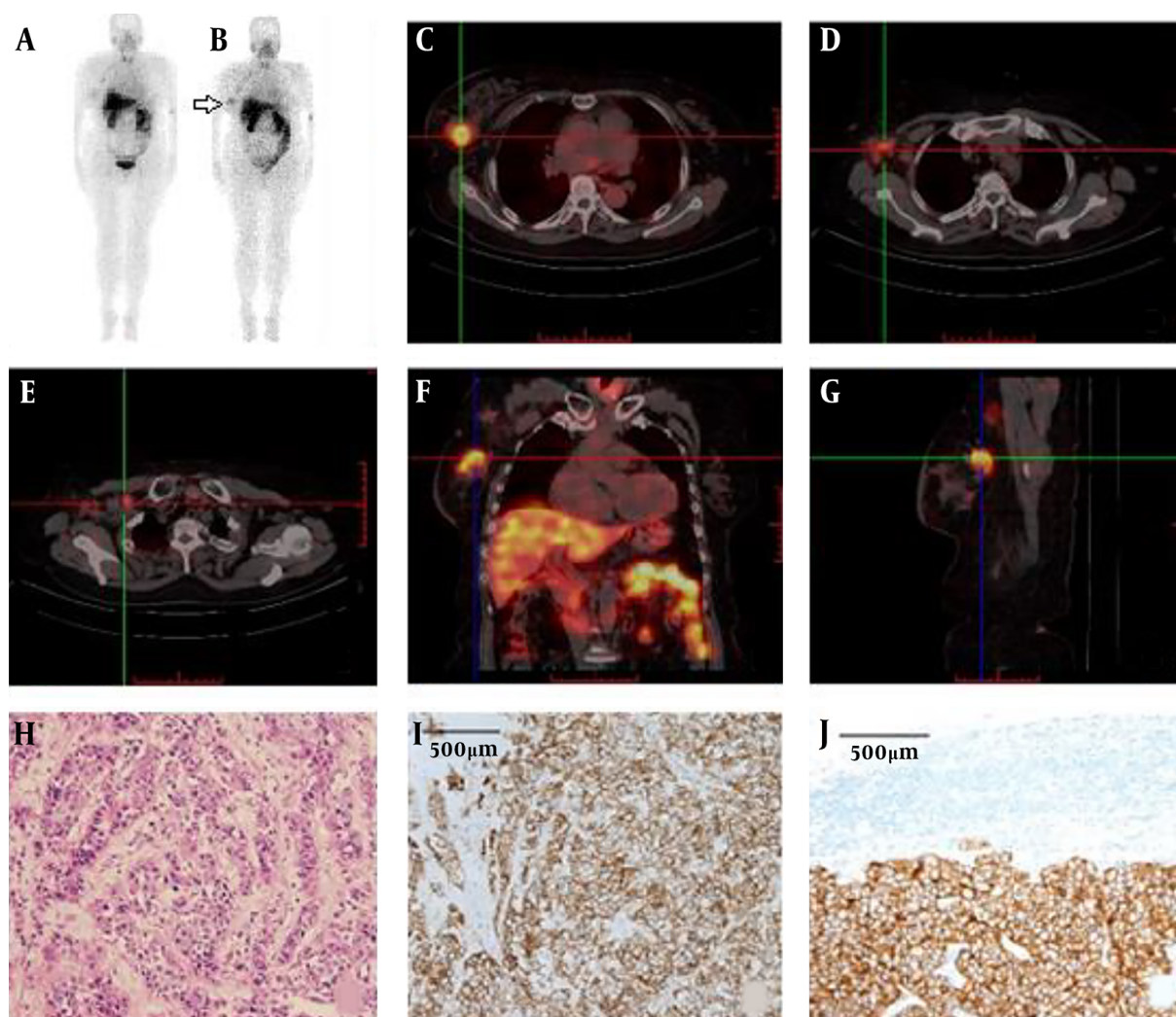


**Figure 2.** Maximum-intensity-projection (MIP) images obtained from patient No. 1 (i.e., at 60 years of age, and body weight (BW) of 70 kg) at 1.5 h (A), and 4.5 h (B) following administration of 370 MBq (50  $\mu$ g) of  $^{99m}\text{Tc}$ -labeled affibody. The breast cancer lesion (C), axillary lymph node (D) and supraclavicular lymph node (E) were clearly visible by transverse plane sectioning. Uptake of non-specific radioactivity by the liver and intestine were noted by coronal plane image analysis (F). The breast cancer lesion displaying human epidermal growth factor receptor 2 (HER2) overexpression was prominent in the sagittal plane (G). All lesions were surgically removed and histologically diagnosed as invasive ductal carcinoma (H). Analysis of HER2 immuno-histochemical staining of the primary tumor (I) and lymph node (J) of patient No. 1, showing (3+) staining intensity.

accumulation of the  $^{99m}\text{Tc}$ -labeled affibody in patient No. 8 was also negligible ( $T/B$  ratio =  $0.3 \pm 0.0$ ) (Figure 3A and C). Follow-up staining by IHC with the HER2-specific antibody confirmed that this invasive lobular carcinoma was negative (Figure 3D).

In Patient No. 26, both  $^{99m}\text{Tc}$ -labeled affibody SPECT and  $^{18}\text{F}$ -FDG PET were undertaken. Bilateral HER2 affibody uptake was visualized (Figure 4A and B); however, only a right faint  $^{18}\text{F}$ -FDG uptake was seen in bilateral breast cancer patients when screened by ultrasound. However, the liver lesions that were identified by  $^{18}\text{F}$ -FDG PET could not be characterized by  $^{99m}\text{Tc}$ -labeled affibody SPECT (Figure 4A

and C).

In the quantitative analysis, a breast lesion with  $^{99m}\text{Tc}$ -labeled affibody uptake that was shown to be 2.4-fold higher than the surrounding muscle ( $T/B \geq 2.4$ ) was arbitrarily considered positive. By contrast, a lesion with a  $T/B < 2.4$  was arbitrarily considered negative. The choice of the threshold was dependent on data listed in Table 2. The nonspecific retention of  $^{99m}\text{Tc}$ -labeled affibody in the liver, spleen and heart limited the application of the tracer in tracing metastasis to these organs, while low accumulation of  $^{99m}\text{Tc}$ -labeled affibody in the muscle and bone would be helpful in identifying metastasis to these tissues

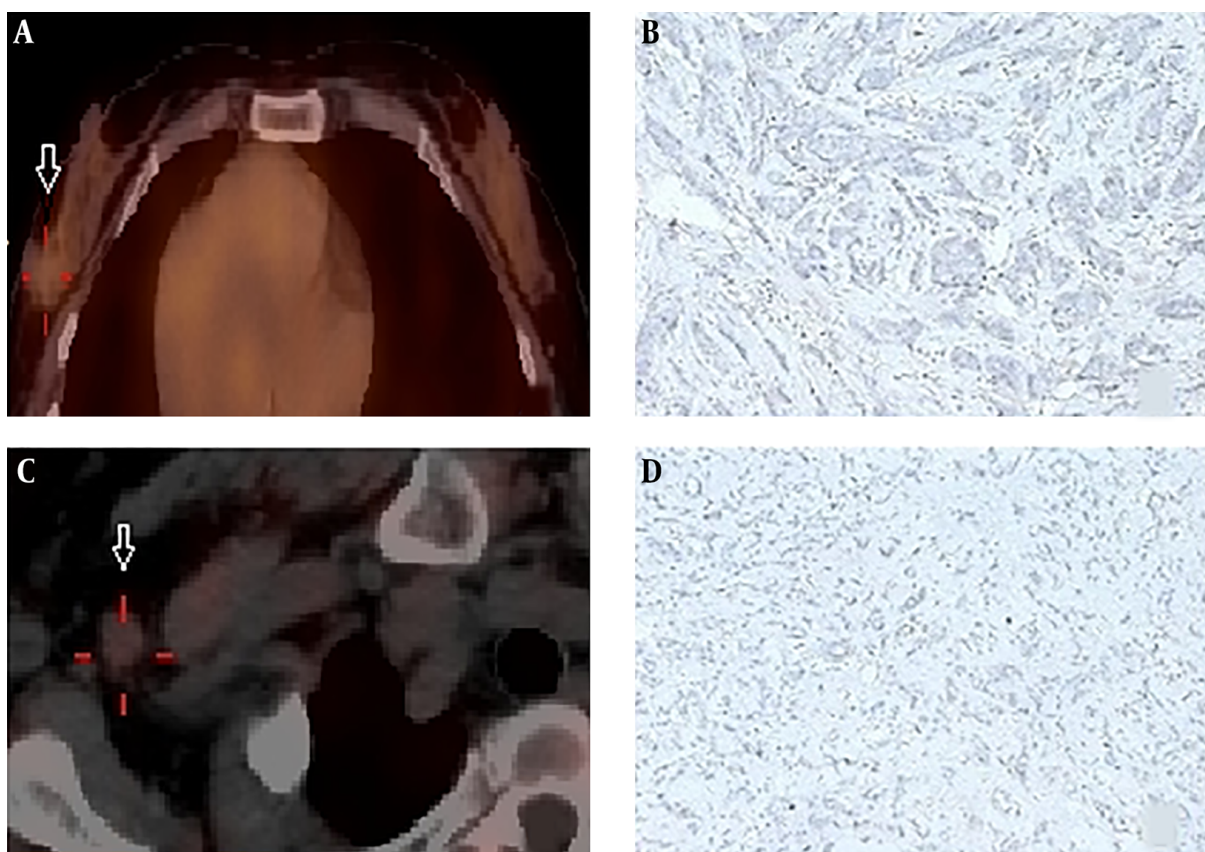


**Figure 3.** Negative image (A) in SPECT with  $^{99m}\text{Tc}$ -labeled affibody in breast cancer lesion of an invasive ductal carcinoma (IDC) (white arrow) patient (No. 22) showed negative pattern of staining in human epidermal growth factor receptor 2 (HER2) immunohistochemistry (B); A patient (No. 8) diagnosed as invasive lobular carcinoma (ILC) also displayed negative uptake with  $^{99m}\text{Tc}$ -labeled affibody (white arrow) (C) and matched negative HER2 expression (D).

**Table 1.** Patient Information and Diagnosis

Demographic information and diagnosis	Values (n = 30)
<b>Age, y</b>	
Range	29 - 76
Mean $\pm$ SD	48.2 $\pm$ 11.1
<b>Diagnosis, %</b>	
Invasive ductal carcinoma (IDC)	83.33
Ductal carcinoma in situ (DCIS)	6.67
Metaplastic breast cancer (MBC)	3.33
Invasive lobular carcinoma (ILC)	3.33
DCIS + IDC	3.33

Abbreviation: SD, standard deviation.

(Figure 5).

#### 4.4. The Correlation Between HER2 Imaging and HER2 IHC

Totally, thirty patients were submitted to  $^{99m}\text{Tc}$ -labeled affibody SPECT/CT imaging, surgery and HER2 IHC staining, and all were included in the correlation analysis. In the IHC

group, 22 patients were HER2 positive, and included the following: 11 patients were scored as HER2 3+, eight patients were scored as HER2 2+ including four FISH positive patients and four FISH negative patients, and three patients were scored as HER2 1+. Additionally, eight patients were found to be HER2 negative (Table 2).

In the HER2 imaging group, 18 patients were identified as HER2 positive and 12 patients were identified as HER2 negative. Six patients that were originally classified as HER2 IHC negative were re-classified as HER2 imaging positive, while three patients that were originally classified as HER2 imaging negative were re-classified as HER2 IHC positive. The HER2 status of the remaining 21 patients was consistent when contrasting HER2 imaging and HER2 IHC (i.e., 12 were true positive and nine were true negative) (Tables 2 and 3). False negativity of HER2 imaging might be related to the tumor size since the diameter of all lesions in three cases was less than 12 mm (i.e., two cases were 10 mm and one case was 11 mm). No false negatives were seen

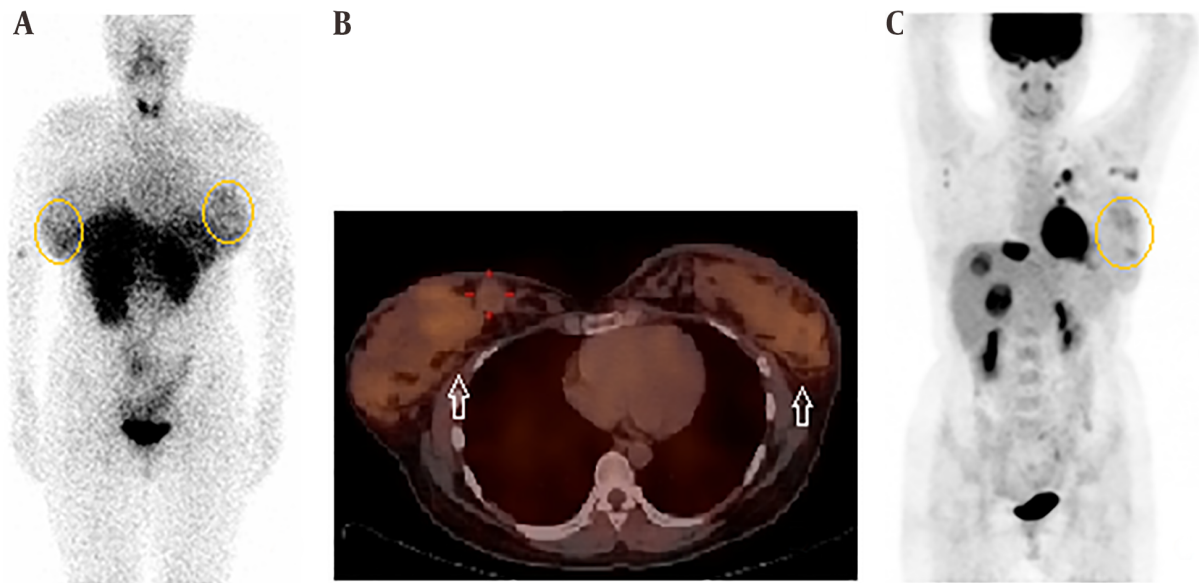


**Figure 4.** Patient No. 26 (invasive ductal carcinoma [IDC]) showed bilateral human epidermal growth factor receptor 2 (HER2) affibody uptake (white arrow) (A, B) and only faint  $^{18}\text{F}$ -fluorodeoxyglucose ( $^{18}\text{F}$ -FDG) uptake was shown on the right (C) by bilateral HER2 positive breast cancer lesions.

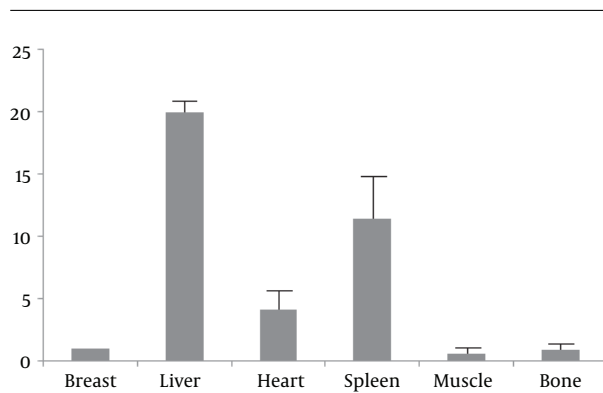


**Figure 5.** The bio-distribution of  $^{99\text{m}}\text{Tc}$ -labeled human epidermal growth factor receptor 2 (HER2) affibody in normal tissues (Y axis: organ or tissue to breast ratio)

when the diameter of the breast cancer lesion was greater than 12 mm, and even a lesion with a size of 13 mm could be accurately stratified—as was the case with patient No.15.

The overall sensitivity, specificity and accuracy were respectively 80 percent (12/15), 60 percent (9/15), and 70 percent (21/30) when the tumor diameter threshold was not set (Table 3). The sensitivity increased to 100 percent (18/18), and the accuracy increased to 84.0 percent (21/25) in examined tumors when the tumor diameter threshold was set as 12 mm.

## 5. Discussion

In our prior studies, HER2 affibody contained an endogenous GGGC chelating sequence that was expressed at the carboxyl-terminus, which was also labeled with technetium-99m giving an RCP that exceeded 95 percent. This was a prerequisite for the current clinical investigation.

In this study, *in vivo* imaging of this type of  $^{99\text{m}}\text{Tc}$ -labeled affibody in breast cancer patients that was examined by SPECT/CT, indicated the feasibility of attempting to clinically translate the endogenously chelating HER2 affibody. The diagnostic sensitivity of  $^{99\text{m}}\text{Tc}$ -labeled affibody could be improved under conditions where tumor size was included during the time of patient enrollment to the study.

However, non-specific retention of  $^{99\text{m}}\text{Tc}$ -labeled affibody in the liver was relatively high, and was secondary to that of the kidneys. The radioactivity in the liver, and kidneys were not ideally cleared from 1.5 to 4.5 hours after  $^{99\text{m}}\text{Tc}$ -labeled affibody administration, which might limit the characterization of HER2 expression following abdominal metastasis of breast cancer (Figure 1A and B). A higher dose might provide improved results and reduced hepatic uptake, which suggested that the dose used in this study needed to be optimized (21).

In the presence of N-terminal HEHEHE modification, the chelator specificity of affibody labeling with  $^{99\text{m}}\text{Tc}$  is partially lost (27). Elevated hepatic uptake as well as uptake

**Table 2.** Patient Diagnosis with HER2 Imaging and Pathological Analysis

PN	CL	LN	H	Pathology (IHC, FISH)	SPECT	SPECT vs. IHC	Size (mm)	T/B
1	R	M	IDC	+(3+)	+	TP	41	23.8
2	L	M	DCIS	+(3+)	-	FN	10	1.8
3	L		IDC	+(3+)	+	TP	26	5.7
4	R		IDC	-(1+)	+	FP	30	4.4
5	L, R		IDC	+(3+)	-	FN	10	1.2
6	R		IDC	-(2+,-)	-	TN	19	2.1
7	R	M	DCIS	+(2+,+)	+	TP	31	4.3
8	R		ILC	-(-)	-	TN	11	0.3
9	R		IDC	-(-)	-	TN	33	2.1
10	R		IDC	-(2+,-)	+	FP	16	12.9
11	L		MBC	-(-)	+	FP	38	5.8
12	R	M	IDC	+(2+,+)	+	TP	27	4.2
13	R		IDC	-(2+,-)	+	FP	14	4.3
14	R		IDC	+(3+)	+	TP	27	3.6
15	L		IDC	+(3+)	+	TP	13	3.9
16	R	M	IDC	+(3+)	+	TP	31	3.5
17	L		IDC	-(-)	-	TN	22	2.2
18	R	M	IDC	+(3+)	+	TP	20	4.2
19	L, R		IDC	-(-)	+	FP	15	4.3
20	L, R		IDC	-(-)	-	TN	16	2.0
21	L	M	DCIS (30% IDC)	-(1+)	+	FP	40	8.6
22	L		IDC	-(-)	-	TN	13	0.8
23	L		IDC	+(3+)	+	TP	50	4.8
24	L	M	IDC	-(1+)	-	TN	27	2.3
25	L, R		IDC	-(-)	-	TN	17	2.1
26	L, R		IDC	+(3+)	+	TP	32	4.9
27	R		IDC	+(3+)	+	TP	24	4.4
28	L, R		IDC	+(2+,+)	+	TP	21	4.7
29	L		IDC	+(2+,+)	-	FN	11	1.9
30	L		IDC	-(2+,-)	-	TN	11	1.4

Abbreviations: CL, cancer location; DCIS, ductal carcinoma in situ; FISH, fluorescence in situ hybridization; FN, false-negative; FP, false-positive; H, histology; HER2, human epidermal growth factor receptor 2; IDC, invasive ductal carcinoma; IHC, immunohistochemistry; ILC, invasive lobular carcinoma; L, left breast; LN, lymph node; M, lymph node metastasis; MBC, metaplastic breast cancer; NA, not applicable; ND, not done; PN, patient number; R, right breast; SPECT, single-photon emission computed tomography; T/B, tumor to background ratio; TN, true negative; TP, true-positive.

in the thyroid might be explained by a suboptimal format of the affibody molecule. The labeling conditions should be optimized in follow-up studies with the intention of reducing the issue of non-specific radioactivity in the liver. We found that renal uptake of <sup>99m</sup>Tc-labeled affibody was the highest, and concordant with similar findings from animal models (35).

From the MIP imaging analysis of the patient, we recog-

nized that the <sup>99m</sup>Tc-labeled affibody was predominantly cleared from the renal - urinary tract, and was secondarily cleared from the hepatic - biliary - gastrointestinal system. The kidneys, urinary bladder, liver, spleen, and intestinal tract all significantly retained the <sup>99m</sup>Tc-labeled affibody. The oral and nasal cavity, salivary glands and thyroid, also showed measurable radioactivity, and the thyroid gland was clearly visible. In addition, the strong digestive uptake

**Table 3.** Quadruple Tabular Form of HER2 Imaging and Pathological Diagnosis<sup>a</sup>

Test standard	Gold standard		Total
	IHC positive	IHC negative	
SPECT positive	12	6	18
SPECT negative	3	9	12
<b>Total</b>	15	15	n = 30

Abbreviations: HER2, human epidermal growth factor receptor 2; IHC, immunohistochemistry; SPECT, single-photon emission computed tomography.

<sup>a</sup>Sensitivity = 80.0%; Specificity = 60%; Accuracy = 70.0%.

of the radioactivity indicated that the free <sup>99m</sup>Tc should be removed completely from the labeling mixture before intravenously administering the construct in future investigations. Moreover, the possible instability of <sup>99m</sup>Tc-labeled affibody could not be ruled out in this study. In this single-center prospective clinical trial, the size of the enrolled and studied patient population was comparatively small. Moreover, follow-up therapy and survival time were not included in this study.

Overall, the low radioactive background in the breast tissue regions allowed detection of HER2 breast cancer lesions with a high target-to-background ratio. In the current study, <sup>99m</sup>Tc-labeled affibody showed improved clinical convenience as defined by ease of labeling, extended biological half-life, and wider availability (36).

Additionally, <sup>99m</sup>Tc-labeled HER2 affibody SPECT/CT imaging of HER2-positive breast cancer might prove useful in the setting of patient stratification for targeted therapy, although we recognize that this approach might exhibit a lower sensitivity for lesion detection as compared with the HER2 affibody PET/CT approach. In addition, we recognize that <sup>99m</sup>Tc-labeled HER2 affibody SPECT/CT imaging of HER2-positive breast cancer performs comparatively poorly in detecting small-sized lesions, hence the use of this approach is not recommended in patients that present with small volume disease.

In a previously published report, the <sup>99m</sup>Tc-labeled tracer showed fewer lesions by SPECT/CT imaging under conditions where the tumor diameter was less than 10 mm (37). The correlation between T/B ratio and HER2 expression in tissues was not statistically significant ( $P = 0.231$ ). This indicated that <sup>99m</sup>Tc-labeled HER2 affibody SPECT imaging was an independent mode of assessment from that provided by HER2 immunohistochemical analysis. The four false positives (out of 30 patients) might mean that IHC missed 13% (4/30) HER2+ breast cancer.

In conclusion, the <sup>99m</sup>Tc labeled HER2 affibody approach was first used to image patients with HER2-positive breast cancer lesions. This approach might also provide imaging guidance for HER2 targeted therapy in breast cancer patients. The non-specific uptake of this radiotracer

in the liver might hamper the detection of HER2 positive liver metastasis in breast cancer. The format of this HER2 affibody molecule, the dose of <sup>99m</sup>Tc-labeled HER2 affibody and the labeling conditions for SPECT/CT imaging in humans should be optimized for future clinical applications.

## Footnotes

**Authors' Contributions:** Study concept and design: Jiong Cai and Pan Wang; analysis and interpretation of data: Xin Li and Feng Mao; drafting of the manuscript: Yaping Luo; critical revision of the manuscript for important intellectual content: Fang Li and Zhaohui Zhu; statistical analysis: Kun Zheng

**Conflict of Interests:** By individual confirmation, it is confirmed that Jiong Cai, Xin Li, Feng Mao, Pan Wang, Yaping Luo, Kun Zheng, Fang Li, and Zhaohui Zhu all declare that they have no conflict of interest with regard this study and its publication.

**Ethical Approval:** All procedures performed in any of the studies reported herein and involving human participants were done in accord with the ethical standards of institutional and/or national research committees and under the auspices of the 1964 Helsinki Declaration and its subsequent amendments or comparable ethical standards.

**Funding/Support:** This study was funded by the National Natural Science Foundation of the Peoples Republic of China, NSFC (grant numbers: 81571712, and 81601551), Zunyi Medical College Research Start Fund 2018ZYFY03, Zhejiang Provincial Medical and Health Science and Technology Plan (grant number: 2017KYB247, Beijing Natural Science Foundation (grant number: 7174338), PUMCH Science Fund of the Key Projects for Junior Faculty (pumch-2016-1.4) and CAMS-12M 2017-12M-3-001).

**Patient Consent:** Informed consent was obtained from all individuals included in this study.

## References

- McGuire A, Brown JA, Malone C, McLaughlin R, Kerin MJ. Effects of age on the detection and management of breast cancer. *Cancers (Basel)*. 2015;7(2):908–29. doi: [10.3390/cancers7020815](https://doi.org/10.3390/cancers7020815). [PubMed: [26010605](https://pubmed.ncbi.nlm.nih.gov/26010605/)]. [PubMed Central: [PMC4491690](https://pubmed.ncbi.nlm.nih.gov/PMC4491690/)].
- Henry KE, Ulaner GA, Lewis JS. Human epidermal growth factor receptor 2-targeted PET/single-photon emission computed tomography imaging of breast cancer: Noninvasive measurement of a biomarker integral to tumor treatment and prognosis. *PET Clin*. 2017;12(3):269–88. doi: [10.1016/j.cpet.2017.02.001](https://doi.org/10.1016/j.cpet.2017.02.001). [PubMed: [28576166](https://pubmed.ncbi.nlm.nih.gov/28576166/)]. [PubMed Central: [PMC5545121](https://pubmed.ncbi.nlm.nih.gov/PMC5545121/)].
- Goldhirsch A, Wood WC, Coates AS, Gelber RD, Thurlimann B, Senn HJ, et al. Strategies for subtypes—dealing with the diversity of breast cancer: Highlights of the St. Gallen International Expert Consensus on the Primary Therapy of Early Breast Cancer 2011. *Ann Oncol*.

- 2011;**22**(8):1736–47. doi: [10.1093/annonc/mdr304](https://doi.org/10.1093/annonc/mdr304). [PubMed: [21709140](https://pubmed.ncbi.nlm.nih.gov/21709140/)]. [PubMed Central: [PMC3144634](https://pubmed.ncbi.nlm.nih.gov/PMC3144634/)].
4. Awada A, Bozovic-Spasojevic I, Chow L. New therapies in HER2-positive breast cancer: A major step towards a cure of the disease? *Cancer Treat Rev*. 2012;**38**(5):494–504. doi: [10.1016/j.ctrv.2012.01.001](https://doi.org/10.1016/j.ctrv.2012.01.001). [PubMed: [22305205](https://pubmed.ncbi.nlm.nih.gov/22305205/)].
  5. Cortes J, Fumoleau P, Bianchi GV, Petrella TM, Gelmon K, Pivot X, et al. Pertuzumab monotherapy after trastuzumab-based treatment and subsequent reintroduction of trastuzumab: Activity and tolerability in patients with advanced human epidermal growth factor receptor 2-positive breast cancer. *J Clin Oncol*. 2012;**30**(14):1594–600. doi: [10.1200/JCO.2011.37.4207](https://doi.org/10.1200/JCO.2011.37.4207). [PubMed: [22393084](https://pubmed.ncbi.nlm.nih.gov/22393084/)].
  6. Murphy CG, Morris PG. Recent advances in novel targeted therapies for HER2-positive breast cancer. *Anticancer Drugs*. 2012;**23**(8):765–76. doi: [10.1097/CAD.0b013e328352d292](https://doi.org/10.1097/CAD.0b013e328352d292). [PubMed: [22824822](https://pubmed.ncbi.nlm.nih.gov/22824822/)].
  7. Verma S, Miles D, Gianni L, Krop IE, Welslau M, Baselga J, et al. Trastuzumab emtansine for HER2-positive advanced breast cancer. *N Engl J Med*. 2012;**367**(19):1783–91. doi: [10.1056/NEJMoa1209124](https://doi.org/10.1056/NEJMoa1209124). [PubMed: [23020162](https://pubmed.ncbi.nlm.nih.gov/23020162/)]. [PubMed Central: [PMC5125250](https://pubmed.ncbi.nlm.nih.gov/PMC5125250/)].
  8. Perez-Trevino P, la Cerda HH, Perez-Trevino J, Fajardo-Ramirez OR, Garcia N, Altamirano J. 3D imaging detection of HER2 based in the use of novel affibody-quantum dots probes and ratiometric analysis. *Transl Oncol*. 2018;**11**(3):672–85. doi: [10.1016/j.tranon.2018.03.004](https://doi.org/10.1016/j.tranon.2018.03.004). [PubMed: [29627705](https://pubmed.ncbi.nlm.nih.gov/29627705/)]. [PubMed Central: [PMC6053773](https://pubmed.ncbi.nlm.nih.gov/PMC6053773/)].
  9. Jahanzeb M. Adjuvant trastuzumab therapy for HER2-positive breast cancer. *Clin Breast Cancer*. 2008;**8**(4):324–33. doi: [10.3816/CBC.2008.n.037](https://doi.org/10.3816/CBC.2008.n.037). [PubMed: [18757259](https://pubmed.ncbi.nlm.nih.gov/18757259/)].
  10. Mates M, Fletcher GG, Freedman OC, Eisen A, Gandhi S, Trudeau ME, et al. Systemic targeted therapy for her2-positive early female breast cancer: A systematic review of the evidence for the 2014 Cancer Care Ontario systemic therapy guideline. *Curr Oncol*. 2015;**22**(Suppl 1):S114–22. doi: [10.3747/co.22.2322](https://doi.org/10.3747/co.22.2322). [PubMed: [25848335](https://pubmed.ncbi.nlm.nih.gov/25848335/)]. [PubMed Central: [PMC4381787](https://pubmed.ncbi.nlm.nih.gov/PMC4381787/)].
  11. Wolff AC, Hammond MEH, Allison KH, Harvey BE, Mangu PB, Bartlett JMS, et al. Human epidermal growth factor receptor 2 testing in breast cancer: American Society of Clinical Oncology/College of American Pathologists clinical practice guideline focused update. *J Clin Oncol*. 2018;**36**(20):2105–22. doi: [10.1200/JCO.2018.77.8738](https://doi.org/10.1200/JCO.2018.77.8738). [PubMed: [29846122](https://pubmed.ncbi.nlm.nih.gov/29846122/)].
  12. Wolff AC, Hammond ME, Hicks DG, Dowsett M, McShane LM, Allison KH, et al. Recommendations for human epidermal growth factor receptor 2 testing in breast cancer: American Society of Clinical Oncology/College of American Pathologists clinical practice guideline update. *J Clin Oncol*. 2013;**31**(31):3997–4013. doi: [10.1200/JCO.2013.50.9984](https://doi.org/10.1200/JCO.2013.50.9984). [PubMed: [24101045](https://pubmed.ncbi.nlm.nih.gov/24101045/)].
  13. Liu YY, Wu SF, Liang ZY, Zeng X. [Comparison of HER2 gene status between primary breast cancer and synchronous axillary lymph node metastasis]. *Zhonghua Bing Li Xue Za Zhi*. 2016;**45**(6):393–6. Chinese. doi: [10.3760/cma.j.issn.0529-5807.2016.06.008](https://doi.org/10.3760/cma.j.issn.0529-5807.2016.06.008). [PubMed: [27256047](https://pubmed.ncbi.nlm.nih.gov/27256047/)].
  14. Erdem GU, Altundag K, Ozdemir NY, Sahin S, Demirci NS, Karatas F, et al. Comparative study of receptor discordance between primary and corresponding metastatic lesions in breast cancer. *J BUON*. 2017;**22**(2):365–76. [PubMed: [28534357](https://pubmed.ncbi.nlm.nih.gov/28534357/)].
  15. Thangarajah F, Vogel C, Pahmeyer C, Eichler C, Holtschmidt J, Ratiu D, et al. Profile and outcome of supraclavicular metastases in patients with metastatic breast cancer: Discordance of receptor status between primary and metastatic site. *Anticancer Res*. 2018;**38**(10):6023–6. doi: [10.21873/anticancer.12952](https://doi.org/10.21873/anticancer.12952). [PubMed: [30275235](https://pubmed.ncbi.nlm.nih.gov/30275235/)].
  16. Alirezapour B, Jalilian AR, Rajabifar S, Mirzaii M, Moradkhani S, Pouladi M, et al. Preclinical evaluation of [(1)(1)(1) In]-DOTA-trastuzumab for clinical trials. *J Cancer Res Ther*. 2014;**10**(1):112–20. doi: [10.4103/0973-1482.131434](https://doi.org/10.4103/0973-1482.131434). [PubMed: [24762497](https://pubmed.ncbi.nlm.nih.gov/24762497/)].
  17. Holloway CM, Scollard DA, Caldwell CB, Ehrlich L, Kahn HJ, Reilly RM. Phase I trial of intraoperative detection of tumor margins in patients with HER2-positive carcinoma of the breast following administration of <sup>111</sup>In-DTPA-trastuzumab Fab fragments. *Nucl Med Biol*. 2013;**40**(5):630–7. doi: [10.1016/j.nucmedbio.2013.03.005](https://doi.org/10.1016/j.nucmedbio.2013.03.005). [PubMed: [23618841](https://pubmed.ncbi.nlm.nih.gov/23618841/)].
  18. Sandstrom M, Lindskog K, Velikyan I, Wennborg A, Feldwisch J, Sandberg D, et al. Biodistribution and radiation dosimetry of the anti-HER2 affibody molecule <sup>68</sup>Ga-ABY-025 in breast cancer patients. *J Nucl Med*. 2016;**57**(6):867–71. doi: [10.2967/jnumed.115.169342](https://doi.org/10.2967/jnumed.115.169342). [PubMed: [26912439](https://pubmed.ncbi.nlm.nih.gov/26912439/)].
  19. Sorensen J, Sandberg D, Sandstrom M, Wennborg A, Feldwisch J, Tolmachev V, et al. First-in-human molecular imaging of HER2 expression in breast cancer metastases using the <sup>111</sup>In-ABY-025 affibody molecule. *J Nucl Med*. 2014;**55**(5):730–5. doi: [10.2967/jnumed.113.131243](https://doi.org/10.2967/jnumed.113.131243). [PubMed: [24665085](https://pubmed.ncbi.nlm.nih.gov/24665085/)].
  20. Baum RP, Prasad V, Muller D, Schuchardt C, Orlova A, Wennborg A, et al. Molecular imaging of HER2-expressing malignant tumors in breast cancer patients using synthetic <sup>111</sup>In- or <sup>68</sup>Ga-labeled affibody molecules. *J Nucl Med*. 2010;**51**(6):892–7. doi: [10.2967/jnumed.109.073239](https://doi.org/10.2967/jnumed.109.073239). [PubMed: [20484419](https://pubmed.ncbi.nlm.nih.gov/20484419/)].
  21. Sorensen J, Velikyan I, Sandberg D, Wennborg A, Feldwisch J, Tolmachev V, et al. Measuring HER2-receptor expression in metastatic breast cancer using [<sup>68</sup>Ga]ABY-025 affibody PET/CT. *Theranostics*. 2016;**6**(2):262–71. doi: [10.7150/thno.13502](https://doi.org/10.7150/thno.13502). [PubMed: [26877784](https://pubmed.ncbi.nlm.nih.gov/26877784/)]. [PubMed Central: [PMC4729774](https://pubmed.ncbi.nlm.nih.gov/PMC4729774/)].
  22. Kurihara H, Hamada A, Yoshida M, Shimma S, Hashimoto J, Yonemori K, et al. (64)Cu-DOTA-trastuzumab PET imaging and HER2 specificity of brain metastases in HER2-positive breast cancer patients. *EJNMMI Res*. 2015;**5**:8. doi: [10.1186/s13550-015-0082-6](https://doi.org/10.1186/s13550-015-0082-6). [PubMed: [25853014](https://pubmed.ncbi.nlm.nih.gov/25853014/)]. [PubMed Central: [PMC4385241](https://pubmed.ncbi.nlm.nih.gov/PMC4385241/)].
  23. Tamura K, Kurihara H, Yonemori K, Tsuda H, Suzuki J, Kono Y, et al. <sup>64</sup>Cu-DOTA-trastuzumab PET imaging in patients with HER2-positive breast cancer. *J Nucl Med*. 2013;**54**(11):1869–75. doi: [10.2967/jnumed.112.118612](https://doi.org/10.2967/jnumed.112.118612). [PubMed: [24029656](https://pubmed.ncbi.nlm.nih.gov/24029656/)].
  24. Mortimer JE, Bading JR, Colcher DM, Conti PS, Frankel PH, Carroll MI, et al. Functional imaging of human epidermal growth factor receptor 2-positive metastatic breast cancer using (64)Cu-DOTA-trastuzumab PET. *J Nucl Med*. 2014;**55**(1):23–9. doi: [10.2967/jnumed.113.122630](https://doi.org/10.2967/jnumed.113.122630). [PubMed: [24337604](https://pubmed.ncbi.nlm.nih.gov/24337604/)]. [PubMed Central: [PMC4084518](https://pubmed.ncbi.nlm.nih.gov/PMC4084518/)].
  25. Zhang JM, Zhao XM, Wang SJ, Ren XC, Wang N, Han JY, et al. Evaluation of <sup>99m</sup>Tc-peptide-ZHER2:342 Affibody® molecule for in vivo molecular imaging. *Br J Radiol*. 2014;**87**(1033):20130484. doi: [10.1259/bjr.20130484](https://doi.org/10.1259/bjr.20130484). [PubMed: [24273251](https://pubmed.ncbi.nlm.nih.gov/24273251/)]. [PubMed Central: [PMC3898972](https://pubmed.ncbi.nlm.nih.gov/PMC3898972/)].
  26. Oroujeni M, Andersson KG, Steinhardt X, Altai M, Orlova A, Mitran B, et al. Influence of composition of cysteine-containing peptide-based chelators on biodistribution of (<sup>99m</sup>Tc)-labeled anti-EGFR affibody molecules. *Amino Acids*. 2018;**50**(8):981–94. doi: [10.1007/s00726-018-2571-1](https://doi.org/10.1007/s00726-018-2571-1). [PubMed: [29728916](https://pubmed.ncbi.nlm.nih.gov/29728916/)]. [PubMed Central: [PMC6060960](https://pubmed.ncbi.nlm.nih.gov/PMC6060960/)].
  27. Lindberg H, Hofstrom C, Altai M, Honorvar H, Wallberg H, Orlova A, et al. Evaluation of a HER2-targeting affibody molecule combining an N-terminal HEHEHE-tag with a GGGC chelator for <sup>99m</sup>Tc-labelling at the C terminus. *Tumour Biol*. 2012;**33**(3):641–51. doi: [10.1007/s13277-011-0305-z](https://doi.org/10.1007/s13277-011-0305-z). [PubMed: [22249974](https://pubmed.ncbi.nlm.nih.gov/22249974/)].
  28. Boswell CA, Brechbiel MW. Development of radioimmunotherapeutic and diagnostic antibodies: An inside-out view. *Nucl Med Biol*. 2007;**34**(7):757–78. doi: [10.1016/j.nucmedbio.2007.04.001](https://doi.org/10.1016/j.nucmedbio.2007.04.001). [PubMed: [17921028](https://pubmed.ncbi.nlm.nih.gov/17921028/)]. [PubMed Central: [PMC2212602](https://pubmed.ncbi.nlm.nih.gov/PMC2212602/)].
  29. Feldwisch J, Tolmachev V, Lendel C, Herne N, Sjoberg A, Larsson B, et al. Design of an optimized scaffold for affibody molecules. *J Mol Biol*. 2010;**398**(2):232–47. doi: [10.1016/j.jmb.2010.03.002](https://doi.org/10.1016/j.jmb.2010.03.002). [PubMed: [20226194](https://pubmed.ncbi.nlm.nih.gov/20226194/)].
  30. Ahlgren S, Orlova A, Wallberg H, Hansson M, Sandstrom M, Lewsley R, et al. Targeting of HER2-expressing tumors using <sup>111</sup>In-ABY-025, a second-generation affibody molecule with a fundamentally reengineered scaffold. *J Nucl Med*. 2010;**51**(7):1131–8. doi: [10.2967/jnumed.109.073346](https://doi.org/10.2967/jnumed.109.073346). [PubMed: [20554729](https://pubmed.ncbi.nlm.nih.gov/20554729/)].
  31. Velikyan I, Schweighofer P, Feldwisch J, Seemann J, Frejd FY, Lindman

- H, et al. Diagnostic HER2-binding radiopharmaceutical, [(68)Ga]Ga-ABY-025, for routine clinical use in breast cancer patients. *Am J Nucl Med Mol Imaging*. 2019;9(1):12-23. [PubMed: 30911434]. [PubMed Central: PMC6420710].
32. Yanai A, Harada R, Iwata R, Yoshikawa T, Ishikawa Y, Furumoto S, et al. Site-specific labeling of F-18 proteins using a supplemented cell-free protein synthesis system and O-2-[(18)F]Fluoroethyl-L-Tyrosine: [(18)F]FET-HER2 affibody molecule. *Mol Imaging Biol*. 2019;21(3):529-37. doi: 10.1007/s11307-018-1266-z. [PubMed: 30112727].
33. Wallberg H, Orlova A, Altai M, Hosseinimehr SJ, Widstrom C, Malmberg J, et al. Molecular design and optimization of 99mTc-labeled recombinant affibody molecules improves their biodistribution and imaging properties. *J Nucl Med*. 2011;52(3):461-9. doi: 10.2967/jnumed.110.083592. [PubMed: 21321280].
34. Cai J, Zheng K, Dang YH, Li F. [Expression and affinity purification of recombinant human epidermal growth factor receptor-2 affibody with C-terminal cystein]. *Zhongguo Yi Xue Ke Xue Yuan Xue Bao*. 2013;35(3):281-5. Chinese. doi: 10.3881/j.issn.1000-503X.2013.03.008. [PubMed: 23827065].
35. Mitran B, Altai M, Hofstrom C, Honarvar H, Sandstrom M, Orlova A, et al. Evaluation of 99mTc-Z IGF1R:4551-GGGC affibody molecule, a new probe for imaging of insulin-like growth factor type 1 receptor expression. *Amino Acids*. 2015;47(2):303-15. doi: 10.1007/s00726-014-1859-z. [PubMed: 25425114]. [PubMed Central: PMC4302241].
36. Andersson KG, Oroujeni M, Garousi J, Mitran B, Stahl S, Orlova A, et al. Feasibility of imaging of epidermal growth factor receptor expression with ZEGFR:2377 affibody molecule labeled with 99mTc using a peptide-based cysteine-containing chelator. *Int J Oncol*. 2016;49(6):2285-93. doi: 10.3892/ijo.2016.3721. [PubMed: 27748899]. [PubMed Central: PMC5118000].
37. Lawal IO, Ankrah AO, Mokgoro NP, Vorster M, Maes A, Sathekge MM. Diagnostic sensitivity of Tc-99m HYNIC PSMA SPECT/CT in prostate carcinoma: A comparative analysis with Ga-68 PSMA PET/CT. *Prostate*. 2017;77(11):1205-12. doi: 10.1002/pros.23379. [PubMed: 28649735].